Non-linear thermal buckling analysis of thin-walled beam structures

Pešić, Igor; Lanc, Domagoj; Turkalj, Goran

NON-LINEAR THERMAL BUCKLING ANALYSIS OF THIN-WALLED BEAM STRUCTURES

I. Pešić[1*] – D. Lanc[1] – G. Turkalj[1]

[1]Department of Engineering Mechanics, Faculty of Engineering, University of Rijeka, Vukovarska 58, 51000 Rijeka

ARTICLE INFO

***Article history*:**
Received: 09.06.2015.
Received in revised form: 20.06.2015.
Accepted: 10.07.2015.

Keywords:
Thermal buckling
Stability
Thin-walled beams
Finite elements

Abstract:

The paper presents an algorithm for thermal buckling analysis of thin-walled beam-type structures. One-dimensional finite element is employed under assumptions of large displacements, large rotation effects but small strains. Stability analysis is performed in load deflection manner using co-rotational formulation. The cross- section mid-line contour is assumed to remain not deformed in its own plane and the shear strains of middle surface are neglected. The material properties of the beam are temperature-dependent. Results are validated on test examples.

1 Introduction

Thin-walled beam structures are commonly very susceptive to buckling failure because of their slenderness [1]. The thermal buckling of such structures has attracted significant attention in the design and analysis of engineering structures in diverse fields such as aerospace engineering, shipbuilding and civil engineering. As a result, many theoretical analyses and experimental investigations have been undertaken on thermal buckling in order to adapt to the fast development and changes in technologies.

The application of the finite element method to the thermal analysis of structures has received considerable attention in the past. Thornton [2] studied the basic problems of complex computer analyses as they relate to the aerospace thermal structural behavior. Snyder and Bathe [3] presented an effective solution procedure for finite element thermo-elastic-plastic and creep analysis with temperature-dependent material properties. Kojić and Bathe [4] presented an algorithm for stable and accurate computations of stresses in finite element thermo-elastic-plastic and creep analysis of metal.

Xue et al. [5] presented a thin-walled beam element for transient temperature analysis of large space structures. Duan et al. [6] derived a beam element for the thermal–dynamic coupling analysis by the updated Lagrangian formulation. Avsec and Oblak [7] investigated the impacts exerted by the temperature field in beams on vibrations of beams. Cui and Hu [8] dealt with thermal buckling and the natural vibration of a simply supported slender beam, which is subject to a uniformly distributed heating and has a frictional sliding end within a clearance.

Cisternas and Holmes [9] studied the bifurcations of the resulting equilibrium equations under both traction and displacement boundary conditions and determined both sub- and supercritical pitchfork bifurcations. Saha and Ali [10] presented an exact mathematical model for the post-buckling of a uniformly heated slender rod with axially immovable simply supported ends on the basis of geometrically non-linear theory of extensible rods. Li and Dong [11] studied fire-induced vibration of full-scale continuous panels using Hilbert transform.

[*] Corresponding author. Tel.: +385 51 651 503; fax: +385 51 651 490
E-mail address: ipesic@riteh.hr

If the thermal effects are ignored, the geometric nonlinear analysis of beam structures is a highly classical problem, which has attracted numerous researchers [12-17]. Belitschko and Hsieh [12] explored the use of convected coordinate procedures, in which each element is associated with coordinate system that rotates but does not deform with the element. Izzuddin and Elnashai [13,14] presented corotational formulation for modeling the effects of large displacements on the response of space frames subjected to conservative loading. Turkalj et al. [15, 16] developed the external stiffness approach to the geometric non-linear analysis of thin-walled frames. Lanc et al. [17] presented a one-dimensional finite element for creep buckling analysis of structures comprised of straight and prismatic beam members.

This paper presents a finite element model for thermal buckling analysis of 3D framed structures with thin-walled open cross section. The model predicts structural response under conditions of extreme mechanical and thermal loading and it takes into account the actual temperature-dependent behavior of material, i.e., decreased moduli with heating. The beam cross-section geometry is discretized by quadratic monitoring areas and the structural discretization is performed throughout one-dimensional finite element. The co-rotational description used in this work is linear on the element level and all geometrically non-linear effects are introduced through the transformation from the local to the global coordinate system. The model is applicable to any shape of the cross section and boundary conditions.

The method is based on premise that forces act on the construction static so that kinetic energy is zero. In that case, total work of outside forces is equal to the potential energy of construction deformation. The material is assumed to be isotropic and linearly elastic. Displacements and rotations are allowed to be large but strains are small. External load is assumed to be conservative, while internal moments are represented by the St. Venant theory of torsion and the Euler-Bernoulli theory of bending.

Verification examples utilizing a numerical algorithm and developed on the basis of abovementioned procedure are presented to demonstrate accuracy of this model.

2 Theoretical background

2.1 Kinematics

In a local Cartesian coordinate system in which beam axis that connects all cross sectional centers of gravity coincides with z axis while x and y are principal axes, whose cross sectional rigid body displacements are:

$$\begin{aligned} &w_0 = w_0(z), \quad u_0 = u_0(z), \quad v_0 = v_0(z), \\ &\varphi_z = \varphi_z(z), \quad \varphi_x = -\frac{dv_0}{dz}, \quad \varphi_y = \frac{du_0}{dz}, \\ &\theta = -\frac{d\varphi_z}{dz}. \end{aligned} \tag{1}$$

In equations above, w_o, u_0 and v_o are the rigid body translations in the z, x and y directions, respectively; while φ_z, φ_x and φ_y are the rigid body rotations around z, x and y axes, respectively. Displacement θ is a cross-sectional warping parameter. The displacement components of an arbitrary point of the cross section are defined as:

$$\begin{aligned} w &= w_o - y\frac{\mathrm{d}v_0}{\mathrm{d}z} - x\frac{\mathrm{d}u_0}{\mathrm{d}z} - \omega\frac{\mathrm{d}\varphi_0}{\mathrm{d}z}, \\ u &= u_0 - y\,\varphi_z, \\ v &= v_0 + x\,\varphi_z \end{aligned} \tag{2}$$

where x and y define the position of the cross section, while ω is a value of the cross-sectional warping function. The strain tensor components can be written as:

$$\varepsilon_z = \frac{\mathrm{d}w_o}{\mathrm{d}z} - y\frac{\mathrm{d}\varphi_x}{\mathrm{d}z} - x\frac{\mathrm{d}\varphi_y}{\mathrm{d}z} - \omega\frac{\mathrm{d}^2\varphi_z}{\mathrm{d}z^2} + \frac{1}{2}\left(x^2 + y^2\right)\left(\frac{\mathrm{d}\varphi_z}{\mathrm{d}z}\right)^2 \tag{3}$$

$$\varepsilon_{zs} = 2n\frac{\mathrm{d}\varphi_z}{\mathrm{d}z}, \tag{4}$$

where s is a circumferential coordinate and n is a normal coordinate in a coordinate system which is introduced into the middle contour of the cross section.

2.2 Stress resultants

The constitutive equations are:

$$\begin{pmatrix} \sigma_z \\ \tau_{zs} \end{pmatrix} = \begin{pmatrix} E & 0 \\ 0 & G \end{pmatrix} \cdot \begin{pmatrix} \varepsilon_z \\ \gamma_{zs} \end{pmatrix} \tag{5}$$

where E and G are the elastic and shear moduli, respectively. Integrating over the contour thickness *n* and the contour direction *s*, and transforming into the beam coordinate system, it follows that the cross-sectional internal force components are:

$$\begin{aligned} F_z &= \int_A \sigma_z \, \mathrm{d}A, \quad M_x = \int_A \sigma_z y \, \mathrm{d}A, \\ M_y &= -\int_A \sigma_z x \, \mathrm{d}A, \quad M_z = \int_A \tau_{zs} n \, \mathrm{d}A, \\ M_\omega &= \int_A \sigma_z \omega \mathrm{d}A, \quad T_\sigma = \int_A \sigma_z \left(x^2 + y^2\right) \mathrm{d}A \end{aligned} \tag{6}$$

where F_z represents the axial force, F_x and F_y are shear forces, M_z is the St. Venant torsion moment, M_x and M_y are bending moments with respect to the *x* and *y* axes, respectively, M_ω is the bi-moment and T_ω is Wagner coefficient. Shear forces are treated as reactive ones so that they can be determined as $F_x = -\mathrm{d}M_y/\mathrm{d}z$ and $F_y = \mathrm{d}M_x/\mathrm{d}z$.

3 Beam finite element

In Fig. 1 two-nodded beam finite element with eight degrees of freedom is presented.

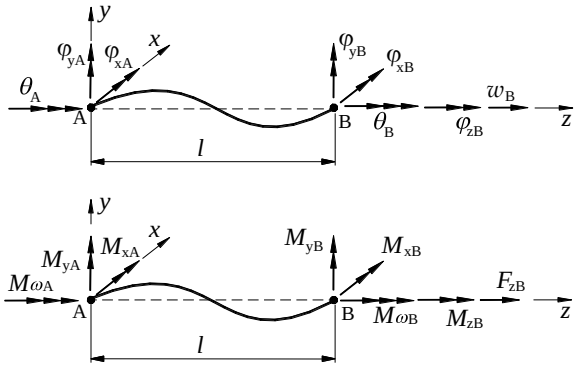

Figure 1. Two-nodded spatial beam element in local coordinate system.

The nodal displacement vector of the beam element is:

$$\left(\mathbf{u}^e\right)^{\mathrm{T}} = \left\{w_{\mathrm{B}}, \varphi_{\mathrm{zB}}, \varphi_{\mathrm{xA}}, \varphi_{\mathrm{xB}}, \varphi_{\mathrm{yA}}, \varphi_{\mathrm{yB}}, \theta_{\mathrm{A,}}, \theta_{\mathrm{B}}\right\}. \tag{7}$$

An appropriate nodal force vector is:

$$\left(\mathbf{f}^e\right)^{\mathrm{T}} = \left\{F_{\mathrm{zB}}, M_{\mathrm{zB}}, M_{\mathrm{xA}}, M_{\mathrm{xB}}, M_{\mathrm{yA}}, M_{\mathrm{yB}}, \mathrm{M}_{\omega\mathrm{A}}, \mathrm{M}_{\omega\mathrm{B}}\right\} \tag{8}$$

and an appropriate thermal nodal force vector is:

$$\left(\mathbf{f}_{\mathrm{t}}^{\mathrm{e}}\right)^{\mathrm{T}} = \left\{\left(EA \cdot \alpha_{\mathrm{t}} \cdot \Delta T\right), 0, 0, 0, 0, 0\right\}, \tag{9}$$

where α_{t} denotes the coefficient of thermal expansion and ΔT is the temperature change.

Incremental analysis supposes that a load-deflection path is subdivided into a number of steps or increments. This path is usually described using three configurations: the initial or undeformed configuration C_0; the last calculated equilibrium configuration C_1 and current unknown configuration C_2. Adopting co-rotational formulation, all system quantities should be referred to configuration C_2. Applying the virtual work principle and neglecting the body forces, the equilibrium of a finite element can be expressed as:

$$\delta U = \delta W, \tag{10}$$

in which *U* is potential energy of internal forces, *W* is the virtual work of external forces, while δ denotes virtual quantities. After making the first variation of Eq. (6), the following incremental equations can be obtained:

$$\delta W = \left(\delta \mathbf{u}^e\right)^{\mathrm{T}} \mathbf{f}^e; \quad \delta U = \left(\delta \mathbf{u}^e\right)^{\mathrm{T}} \mathbf{k}_{\mathrm{T}}^e \mathbf{u}^e. \tag{11}$$

In Equation (11), $\mathbf{k}_{\mathrm{T}}^e$ denotes the local tangent stiffness matrix of the *e*-th beam element, which can be evaluated according to the procedure explained in references [14, 17]. Now the incremental equilibrium equation can be written in the following form:

$$\mathbf{k}_{\mathrm{T}}^{\mathrm{e}} \Delta \mathbf{u}^{\mathrm{e}} = \Delta \mathbf{f}^{\mathrm{e}} - \Delta \mathbf{f}_t^e. \tag{12}$$

The element global tangent stiffness matrix $\overline{\mathbf{k}}_{\mathrm{T}}^e$ can be obtained as follows:

$$\bar{\mathbf{k}}_{\mathrm{T}}^{e} = \mathbf{t}_1^e \mathbf{k}_{\mathrm{T}}^{e} \mathbf{t}_1^e + \mathbf{t}_2^e \mathbf{f}^e \tag{13}$$

Matrices $\mathbf{t}_1^e$ and $\mathbf{t}_2^e$ are standard transformation matrices from local co-rotational to global coordinate system explained in reference [14]. Matrix $\mathbf{t}_1^e$ is of dimension 14×8 and contains first derivations of local with respect to global displacements, while $\mathbf{t}_2^e$ is 14×14×8 matrix containing second derivations. Matrix $\mathbf{t}_2^e$ presents geometric stiffness contribution because it contains effects on global forces caused with change in geometry. The element force vector transformed from the local to global coordinate system is:

$$\bar{\mathbf{f}}^{e} = \mathbf{t}_1^e \mathbf{f}^{e}. \tag{14}$$

After the standard assembling procedure, the overall incremental equilibrium equations can be obtained as:

$$\mathbf{K}_{\mathrm{T}}\mathbf{U} = \mathbf{P}, \quad \mathbf{K}_{\mathrm{T}} = \sum_{e} \bar{\mathbf{k}}_{\mathrm{T}}^{e}, \quad \mathbf{P} = {}^{2}\mathbf{P} - {}^{1}\mathbf{P}, \tag{15}$$

where $\mathbf{K}_{\mathrm{T}}$ is tangential stiffness matrix of a structure, while $\mathbf{U}$ and $\mathbf{P}$ are the incremental displacement vector and the incremental external loads of the structure, respectively. ${}^{2}\mathbf{P}$ and ${}^{1}\mathbf{P}$ are the vectors of external loads applied to the structure at C_2 and C_1 configurations, respectively.

4 Numerical examples

4.1 Channel-section beam

Thermal buckling of uniformly heated simply supported beam has been considered (Fig. 2). The beam length is L = 4 m and thin-walled channel-section corresponding to UPN50x25 is analyzed. The material properties are: elastic modulus E = 210 GPa, Poisson's ratio ν = 0.3 and coefficient of thermal expansion α_t = 1.25·10-5 1/°C. To initiate the occurrence of buckling, a horizontal perturbation force $\Delta F = 0.001 F_{cr}$ acting in the positive X axis direction is added in the middle of the beam. The beam is discretized with four beam finite elements.

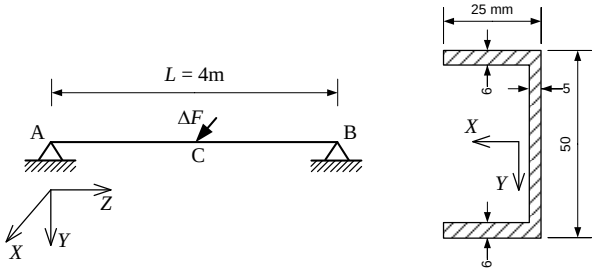

Figure 2. Simply supported beam and cross-section geometry.

The thermal buckling occurs as a result of the thermal stress increase. Since the temperature rise is low, it has no influence on the mechanical behavior of the beam. Fig. 4 shows the relation between temperature change and displacement of point C in perturbation force direction. Theoretical value of critical buckling load F_{cr} = 3225.5 N occurs at ΔT_{cr} = 2.5°C.

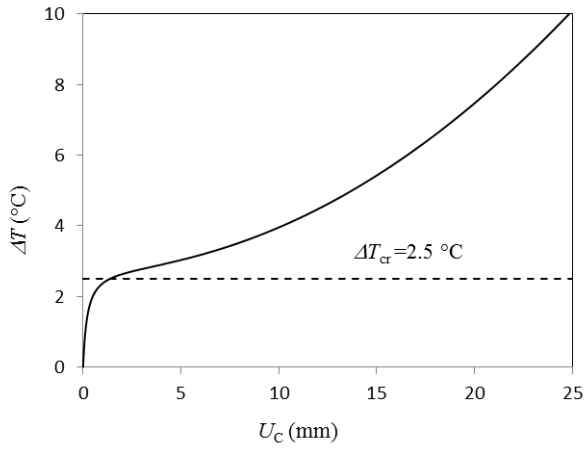

Figure 3. Temperature change vs. displacement.

Buckling predictions in this paper show that very good accuracy is achieved in comparison with theoretical result marked with a dashed line.

4.2 I-beam cantilever

This problem is concerned with thermal buckling of a wide flange cantilever made of 20MnCr5 steel. Fig. 4 shows an axially loaded cantilever perturbated with ΔF = 0,001F acting in the X-axis direction at the point B. The cantilever length is L = 4 m. Mesh configuration of 4 beam elements is used.

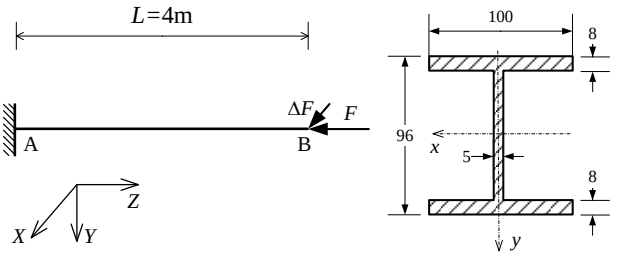

Figure 4. Axially loaded I-beam cantilever.

The cantilever is subjected simultaneously to thermal and mechanical load. In this case, the temperature rise degrades the material properties to withstand loads. Since the temperature is high, Young's modulus is significantly reduced and that causes thermal buckling. The effect of temperature on mechanical properties of 20MnCr5 steel is examined by Brnić et al. [18]. Temperature dependence of the elastic modulus is given by this polynomial approximation:

$$E(T) = 3.45 \cdot 10^{-9} T^4 - 5.47 \cdot 10^{-6} T^3 + 2.43 \cdot 10^{-6} T^2 - 4.68 \cdot 10^{-1} T + 229.12 \quad (16)$$

Fig. 5 shows the relation between applied load and cantilever tip displacement in the *X*-axis. Theoretical value of critical buckling load at 20 °C is 45.06 kN and 27.56 kN at 500 °C. Results are in good agreement with the theoretical value of critical buckling load at 500 °C.

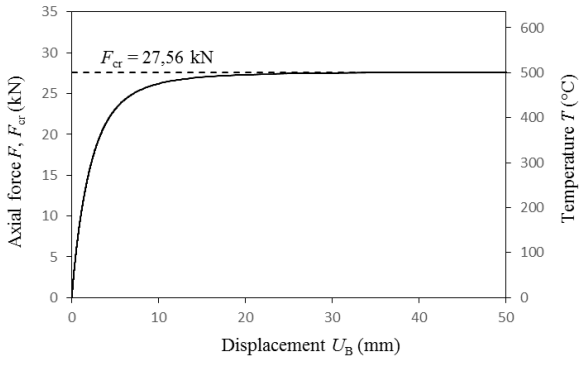

Figure 5. Load and temperature vs. displacement curves for cantilever.

4.3 Space frame

Fig. 13 shows a one-story space frame loaded by four vertical forces, each of intensity *F*, at the corners. The sway instability mode of the frame is analyzed. Two perturbation forces acting in positive *X*-axis direction, each of intensity $\Delta F = 0{,}001F$, are added at corners A and D in order to initiate sway buckling mode of space frame. Both columns and girders have a cruciform cross-section. The full warping restrain is assumed to exist at the ends of each frame member. Each frame leg is discretized by four beam finite elements of equal length. Analyzed material is X10CrAlSi25 steel. Temperature dependence of the elastic modulus is given by this polynomial approximation [19]:

$$E(T) = 2.42 \cdot 10^{-7} T^3 - 4.65 \cdot 10^{-4} T^2 + 3.02 \cdot 10^{-2} T + 190.8 \quad (17)$$

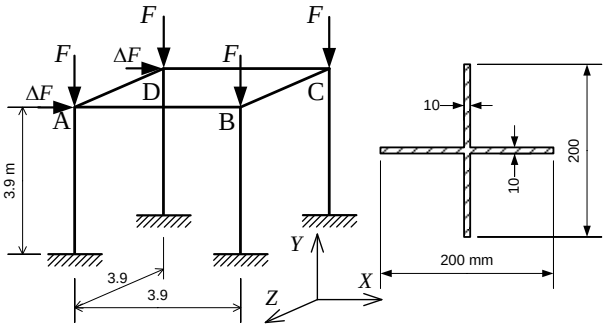

Figure 6. One-story space frame.

The failure of structure is caused by the material degradation at elevated temperature. The critical buckling loads have been determined with linear shell model in Nastran using 4288 finite elements (Fig. 7). Buckling load at 20 °C is 691.46 kN and 309.16 kN at 600 °C.

Figure 7. Sway buckling mode – shell model NASTRAN.

The horizontal displacement of the corner B in the *X*-axis direction is depicted in Fig. 8. The results are in good agreement with critical buckling load obtained by NASTRAN.

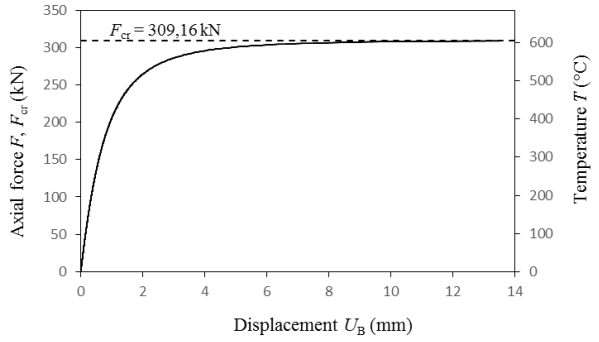

Figure 8. Load and temperature vs. displacement curves for space frame.

5 Conclusion

Co-rotational formulation for the non-linear thermal buckling analysis of beam columns with the thin-walled open cross section is proposed. Material non-linearity is included in the finite element model. The governing incremental equilibrium equations of a two-node space beam element are developed using the linearized virtual work principle. Presented test examples suggest that developed numerical model is an accurate tool for modelling the thermal buckling of the thin-walled beam structures.

Acknowledgement

Authors gratefully acknowledge the financial support given by the Croatian Science Foundation (project No. 6876) and the University of Rijeka (13.09.1.1.03 and 13.09.2.2.20).

References

[1] Alfutov, N.A.: *Stability of Elastic Structures*, Springer-Verlag, Berlin, 2000.

[2] Thornton, E.A.: *Thermal Structures for Aerospace Applications*, AIAA Education Series, Reston, 1996.

[3] Snyder, M.D., Bathe K.J.: *A solution procedure for thermo-elastic-plastic and creep problems*, Nuclear Engineering and Design, 64 (1981), 1, 49-80.

[4] Kojić, M., Bathe K.J.: *The 'effective-stress-function' algorithm for thermo-elasto-plasticity and creep*, International Journal for Numerical Methods in Engineering, 24 (1987), 8, 1509–1532.

[5] Xue, M.D., Duan, J., Xiang Z.H.: *Thermally induced bending-torsion coupling vibration of large scale space structures*, Computational Mechanics, 40 (2007), 4, 707–723.

[6] Duan, J., Oblak, M.: *Thermal vibrational analysis for simply supported beam and clamped beam*, International Journal of Structural Stability and Dynamics, 8 (2008), 4, 569–596.

[7] Avsec, J., Xiang Z.H., Xue, M.D.: *Thermal-dynamic coupling analysis of large space structures considering geometric nonlinearity*, Journal of Sound and Vibration, 308 (2007), 3-5, 514–525.

[8] Cui, D.F., Hu H.Y.: *Thermal buckling and natural vibration of the beam with an axial stick–slip–stop boundary*, Journal of Sound and Vibration, 333 (2014), 2271–2282.

[9] Cisternas, J., Holmes, P.: *Buckling of extensible thermoelastic rods*, Mathematical and Computer Modelling, 36 (2002), 3, 233–243.

[10] Saha, S., Ali, A.R.Md.: *Thermal Buckling and Postbuckling Characteristics of Extensional Slender Elastic Rods*, Journal of Mechanical Engineering, 40 (2009), 1, 1-8.

[11] Li, B., Dong, L.Y.: *Studies on fire-induced vibration of full-scale continuous panels using Hilbert transform*, Engineering Review, 35 (2015), 1, 1-8.

[12] Belitschko, T., Hsieh, B.J.: *Thermal Buckling and Postbuckling Characteristics of Extensional Slender Elastic Rods*, Journal of Mechanical Engineering, 40 (2009), 1, 1-8.

[13] Izzuddin, B.A., Elnashai, A.S.: *Eulerian formulation for large displacement analysis of space frames*, Journal of Engineering Mechanics, 119 (1993), 549-569.

[14] Izzuddin, B.A.: *Conceptual issues in geometrically nonlinear analysis of 3D framed structures*, Computer Methods in Applied Mechanics and Engineering, 191 (2001), 1029-1053.

[15] Turkalj, G., Brnić, J., Prpić Oršić, J.: *Large rotation analysis of elastic thin-walled beam-type structures using ESA approach*, Computers & Structures, 81 (2003), 1851-1864.

[16] Turkalj, G., Brnić, J.: *Nonlinear analysis of thin-walled frames using UL-ESA formulation*, International Journal of Structural Stability and Dynamics, 4 (2004), 45-67.

[17] Lanc, D., Turkalj, G., Brnić, J.: *Finite-element model for creep buckling analysis of beam-type structures*, Communications in Numerical Methods in Engineering, 24 (2008), 989-1008.

[18] Brnić, J., Niu, J, Turkalj, G., Čanađija, M., Lanc, D., Brčić, M., Kršćanski., S, Vukelić, G.: *Comparison of Material Properties and Creep Behavior of 20MnCr5 and S275JR Steels*, Materials Science Forum, 762 (2013), 47-54.

[19] Brnić, J., Turkalj, G., Kršćanski, S., Lanc, D., Čanađija, M., Brčić, M.: *Information relevant for the design of structure: Ferritic – Heat resistant high chromium steel X10CrAlSi25*, Materials and Design, 63 (2014), 508-518.